nature structural & molecular biology

Interactions between lipids and voltage sensor paddles detected with tarantula toxins

Mirela Milescu[1], Frank Bosmans[1,2], Seungkyu Lee[3], AbdulRasheed A Alabi[1,4], Jae Il Kim[3] & Kenton J Swartz[1]

Voltage-activated ion channels open and close in response to changes in voltage, a property that is essential for generating nerve impulses. Studies on voltage-activated potassium (Kv) channels show that voltage-sensor activation is sensitive to the composition of lipids in the surrounding membrane. Here we explore the interaction of lipids with S1–S4 voltage-sensing domains and find that the conversion of the membrane lipid sphingomyelin to ceramide-1-phosphate alters voltage-sensor activation in an S1–S4 voltage-sensing protein lacking an associated pore domain, and that the S3b–S4 paddle motif determines the effects of lipid modification on Kv channels. Using tarantula toxins that bind to paddle motifs within the membrane, we identify mutations in the paddle motif that weaken toxin binding by disrupting lipid-paddle interactions. Our results suggest that lipids bind to voltage-sensing domains and demonstrate that the pharmacological sensitivities of voltage-activated ion channels are influenced by the surrounding lipid membrane.

Kv channels contain a central pore domain[1,2] that opens and closes in response to conformational changes in the four surrounding voltage-sensing domains[3]. Each subunit in these tetrameric channels has six membrane-spanning segments (S1 through S6), with S1–S4 comprising each voltage-sensing domain and the four S5–S6 regions together forming the central pore domain. X-ray structures of these channels predict that the S1–S4 voltage-sensing domains would be extensively exposed to surrounding lipids when embedded in a membrane[1,4], and functional studies demonstrate that changing the composition of the lipid membrane can have striking effects on how these channels open and close in response to changes in voltage[5–10]. In studies on the KvAP channel from *Aeropyrum pernix* reconstituted in defined lipid membranes, lipids with phosphate-containing head groups are required for channel activation[5], leading to the proposal that arginine residues in the voltage sensor are stabilized in the membrane by interactions with phosphate lipid head groups. Experiments in native lipid membranes[6,7] indicate that the phosphate head group of sphingomyelin has a similar role in the activation of the well-studied Shaker Kv channel from *Drosophila melanogaster*[11] and the mammalian Kv2.1 channel from rat brain[12]. Modification of sphingomyelin does not influence the gating of several other related Kv channels[6], suggesting that there is specificity in the interaction between lipids and Kv channels. In the case of Kv2.1, the effects of modification of sphingomyelin can be diminished by toxins that bind to voltage sensors[7], raising the possibility that sphingomyelin interacts directly with voltage sensors in the channel, perhaps similarly to the non-annular lipids observed for other membrane proteins[13,14]. In the present study we set out to determine whether sphingomyelin interacts with the voltage-sensing domains in Kv2.1 channels and to identify specific regions where the lipid might bind. Our results suggest that sphingomyelin interacts with a particular structural motif within voltage sensors and that these interactions can influence the pharmacological sensitivities of the channel.

RESULTS

We investigated how sphingomyelinase D (SMaseD), an enzyme that converts sphingomyelin to ceramide-1-phosphate, influences the gating and pharmacological sensitivities of the Kv2.1 channel from rat brain[12]. Lu and colleagues reported that this Kv channel is particularly sensitive to the lipase[6], with removal of the choline moiety of sphingomyelin causing the channel to open at voltages at which it would otherwise be closed[6]. Application of SMaseD to the extracellular side of cells expressing Kv2.1 caused a −30-mV shift of the conductance-voltage (G-V) relation (**Fig. 1a**) that developed over 10–15 min and was not reversible over the time frame of our recordings (>1 h), consistent with previous results[6]. Deactivation of the channel following membrane repolarization was greatly slowed after SMaseD treatment (**Fig. 1a**), indicating that the lipid modification causes a pronounced stabilization of the open state of the channel.

Lipid modification alters voltage sensor activation

To explore whether the effects of SMaseD result from interactions between lipids and the S1–S4 voltage-sensing domain of the channel, we asked whether the lipase has similar effects on another protein containing an S1–S4 voltage-sensing domain but lacking a pore domain. For these experiments we used the *Ciona intestinalis* voltage-sensitive

[1]Molecular Physiology and Biophysics Section, Porter Neuroscience Research Center, National Institute of Neurological Disorders and Stroke, National Institutes of Health, Bethesda, Maryland, USA. [2]Laboratory of Toxicology, University of Leuven, Leuven, Belgium. [3]Department of Life Sciences, Gwangju Institute of Science and Technology, Gwangju, Korea. [4]Present address: Department of Molecular and Cellular Physiology, Stanford University, Stanford, California, USA. Correspondence to M.M. (Mirela.Milescu@nih.gov) or K.J.S. (Kenton.Swartz@nih.gov).

Received 20 May; accepted 12 August; published online 27 September 2009; doi:10.1038/nsmb.1679

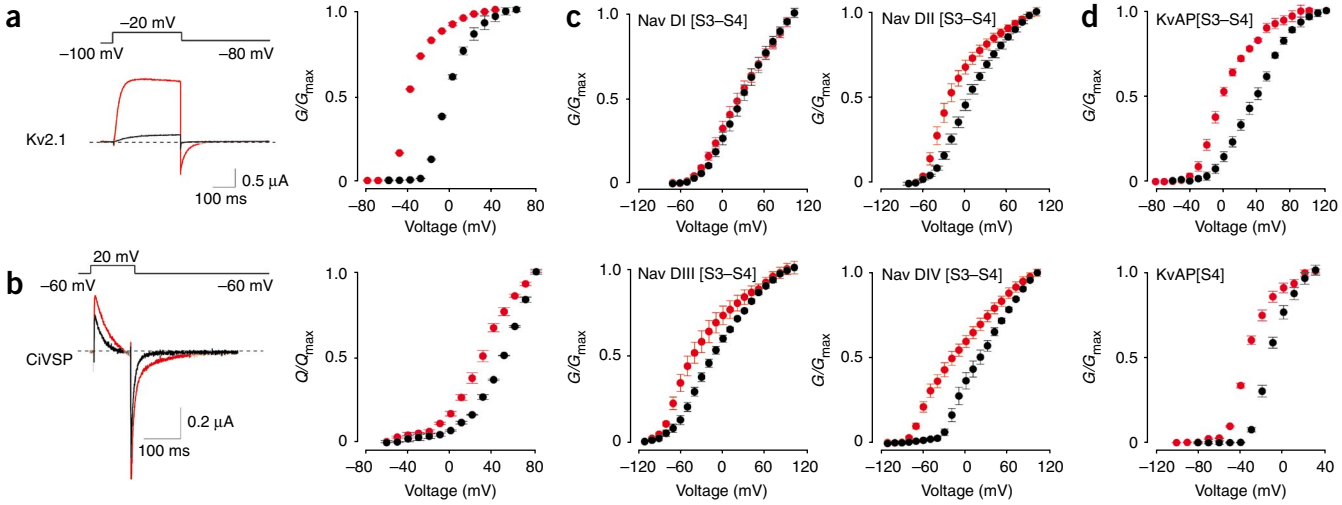

Figure 1 Membrane modification alters gating of voltage-activated ion channels and a voltage-activated phosphatase. G-V and Q-V relations obtained for native membranes are shown in black, and those after treatment with SMaseD are shown in red. (**a**) Ionic current traces and G-V relations for Kv2.1. (**b**) Gating current traces and Q-V relations for Ci-VSP. (**c**) G-V curves for Kv2.1 chimeras that contain individual paddle motifs from each of the four domains of rNav1.4. The holding voltage was –100mV for the Nav DI and Nav DII chimeras and –120mV for the Nav DIII and NavDIV chimeras, the test pulse duration was 300 ms (500 ms for Nav DIV) and the tail voltage was –60mV for Nav DI, –80mV for Nav DII, –110mV for Nav DIII and –100mV for Nav DIV. (**d**) G-V curves for chimeras where complete (S3-S4) or partial (S4) paddle motifs of Kv2.1 were replaced with homologous regions from KvAP. The holding voltage was –100mV, the test pulse duration was 300 ms and the tail voltage was –80mV. In all cases conductance was determined from normalized tail currents. For ionic currents, leak, background and capacitive currents were isolated and subtracted after blocking the Kv channels with agitoxin-2; for gating currents, they were subtracted using a P/–4 protocol. Error bars indicate s.e.m. ($n = 3$).

phosphatase (Ci-VSP), which contains a cytoplasmic phosphatase domain rather than a transmembrane pore[15], and monitored activation of its S1–S4 voltage-sensing domain by measuring charge movement in response to membrane depolarization[15–17]. Extracellular application of SMaseD to cells expressing Ci-VSP produced an approximately –20-mV shift of the charge-voltage (Q-V) relationship to more negative voltages (**Fig. 1b**). As in the case of Kv2.1, the effects of the enzyme developed over 10–15 min and were effectively irreversible. These results demonstrate that modification of sphingomyelin can influence the activity of S1–S4 voltage-sensing domains in the absence of a pore domain.

S3b–S4 paddles determine the effects of lipid modification

One interesting candidate for a region within S1–S4 voltage-sensing domains that interacts with lipids is the S3b–S4 paddle motif, a helix-turn-helix motif that moves in contact with the lipid membrane to sense changes in voltage[3,4,8,18–22]. To explore the possibility that sphingomyelin interacts with the paddle motif, we measured the effects of SMaseD on Kv2.1 chimeras containing paddle motifs from various voltage-activated ion channels (**Fig. 1c**,**d**). Of the constructs we studied, those containing paddle motifs from the four different voltage-sensing domains of the rat skeletal muscle Nav1.4 sodium channel[23] were the most informative. These Nav channel paddle motifs were capable of gating the Kv2.1 channel and rendering the Kv channel sensitive to Nav channel toxins[21]; however, SMaseD altered the G-V relations of the chimeras to different extents (**Fig. 1d**). In particular, Kv channels containing the paddle motif from domain I of Nav1.4 were effectively insensitive to SMaseD, suggesting that the paddle motifs determine the sensitivity of the channel to lipid modification.

Lipid modification alters voltage sensor pharmacology

If the membrane lipids studied here actually bind to paddle motifs in Kv channels, it is possible that the binding of other ligands at the protein-lipid interface would be influenced by lipid modification. Because tarantula toxins partition into membranes[9,24–26] (**Supplementary Fig. 1**) and bind to regions of the paddle motif facing the surrounding membrane[1,8,10,21,27–29], we investigated whether their interaction with the paddle motif is altered by lipid modification. We studied the effects of SMaseD on the interaction of the GxTx-1E[30] toxin with the wild-type Kv2.1 channel, VSTx1 (refs. 25,31) with a chimera produced by transplanting the S4 helix from KvAP into Kv2.1 (KvAP[S4])[8] and ProTx-I[32] with the two Nav paddle chimeras that are sensitive to the toxin[21] (**Fig. 2**). The lipid modification produced a 3.9-fold increase in the apparent affinity of GxTx-1E for Kv2.1 (**Fig. 2a**) and a 6.2-fold increase in that of VSTx1 for the KvAP chimera (**Fig. 2b**). The effects of ProTx-I on the two Nav paddle chimeras are particularly noteworthy, as the apparent affinity of the toxin is increased by only 50% for the domain II chimera (Nav DII [S3-S4]) but by more than six-fold for the domain IV chimera (Nav DIV [S3–S4]) (**Fig. 2c**,**d**). These effects of SMaseD on the interactions of tarantula toxins with paddle motifs demonstrate that the toxins can sense the lipid modification.

The distinct effects of the lipase on ProTx-I interaction with the two Nav paddle chimeras suggest that the modification does not simply alter the way these toxins interact with lipids (for example, by altering the toxin concentration in the membrane) but that the toxins can actually detect differences in the way lipids interact with distinct paddle motifs. To confirm that partitioning of tarantula toxins is not altered by SMaseD, we compared partitioning of ^{125}I-GxTx-1E into intact oocyte membranes[9] before and after lipid modification. At a concentration of GxTx-1E (200 nM) that completely inhibited opening of Kv2.1 (**Fig. 2a**), partitioning of the toxin was unaffected by SMaseD treatment (**Fig. 2e**).

Tarantula toxins detect lipid-paddle interactions

Previous studies have shown that tarantula toxins interact with the paddle motif in a specific fashion, with mutations in the

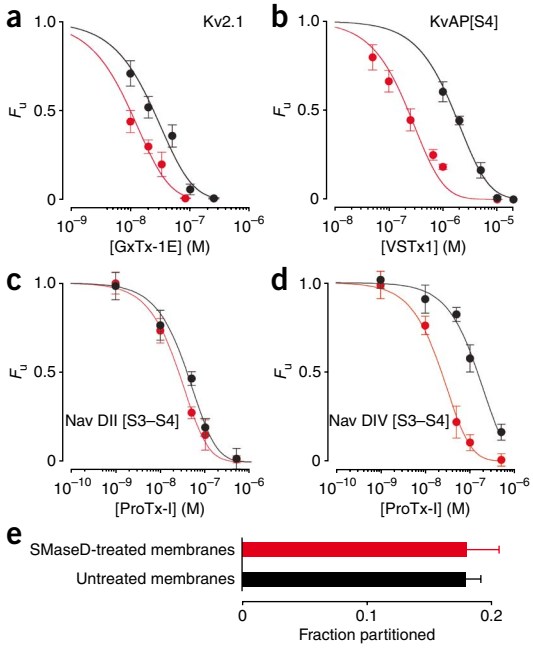

Figure 2 Membrane modification alters the apparent affinity of tarantula toxins for Kv channels without altering membrane partitioning. (**a**–**d**) Concentration dependence for tarantula toxin occupancy of wild-type and chimeric Kv channels, before (black) and after (red) SMaseD treatment. F_u represents the fraction of unbound channels and was estimated from fractional inhibition at negative voltages (see Online Methods and **Supplementary Fig. 5**). Smooth curves represent fits of $F_u = ([Toxin]/([Toxin] + K_d))^4$ to the data. The apparent K_d values for the toxin-channel pairs before and after SMaseD treatment are 203 ± 38 nM and 52 ± 8 nM for GxTx-1E and Kv2.1 (**a**) and 10 ± 2.5 μM and 1.6 ± 0.3 μM for VSTx1 and KvAP[S4] (**b**), 210 ± 9 nM and 137 ± 9 nM for ProTx-I and Nav DII [S3–S4] (**c**) and 780 ± 77 nM and 122 ± 7 nM for ProTx-I and Nav DII [S3-S4] (**d**). n = 3–5 for each toxin concentration and error bars indicate s.e.m. At a concentration of 100 nM, ProTx-I had no effect on Nav DI [S3–S4] and Nav DIII [S3–S4] chimeras. (**e**) Partitioning of ^{125}I-GxTx-1E into oocyte membranes before (black) and after (red) treatment with SMaseD. Error bars indicate s.e.m. (n = 5).

paddle having pronounced effects on the apparent affinity of these toxins[8,10,21,26,27,29,33]. The idea that both lipids and toxins interact with the the paddle motif raises the intriguing possibility that mutations in the paddle might alter toxin affinity by disrupting lipid-paddle interactions. In search of such mutations, we substituted each residue in the paddle motif of Kv2.1 with alanine and measured the apparent affinity of GxTx-1E for these channels in control membranes and after treatment with SMaseD. Mutations such as V282A and E277A decreased the apparent affinity of the toxin when studied in untreated membranes, but did so to a lesser extent after lipid modification (**Fig. 3a**). In the case of V282A, the mutant weakened toxin affinity by more than 18-fold under control conditions, but by only about two-fold after treatment with the lipase. In this instance, the extent to which the mutation weakens toxin affinity is markedly dependent on the lipids around the channel, suggesting that the mutation actually influences how lipids interact with the paddle motif. Another way of looking at this result is to consider that for the wild-type channel lipid modification increased toxin affinity by only about four-fold; however, after the paddle mutation is introduced, weakening toxin binding, addition of the lipid modification increased toxin affinity by more than 30-fold (**Fig. 3a**, **Supplementary Fig. 2** and **Supplementary Tables 1** and **2**). Thus, it seems that the lipid modification can correct the disruptive effects of the mutation (see Discussion).

The E277A mutant is an example where the effect of the mutation on toxin affinity is moderately different between control and SMaseD-treated membranes, even though the mutant alters the affinity of the toxin by almost 150-fold when studied in control membranes (**Fig. 3a**). In this instance, the mutant seems to weaken toxin affinity largely by altering a protein-protein interaction, and the lipid modification can only modestly correct the effects of the mutation. The extent to which the lipid modification and paddle mutations are coupled can

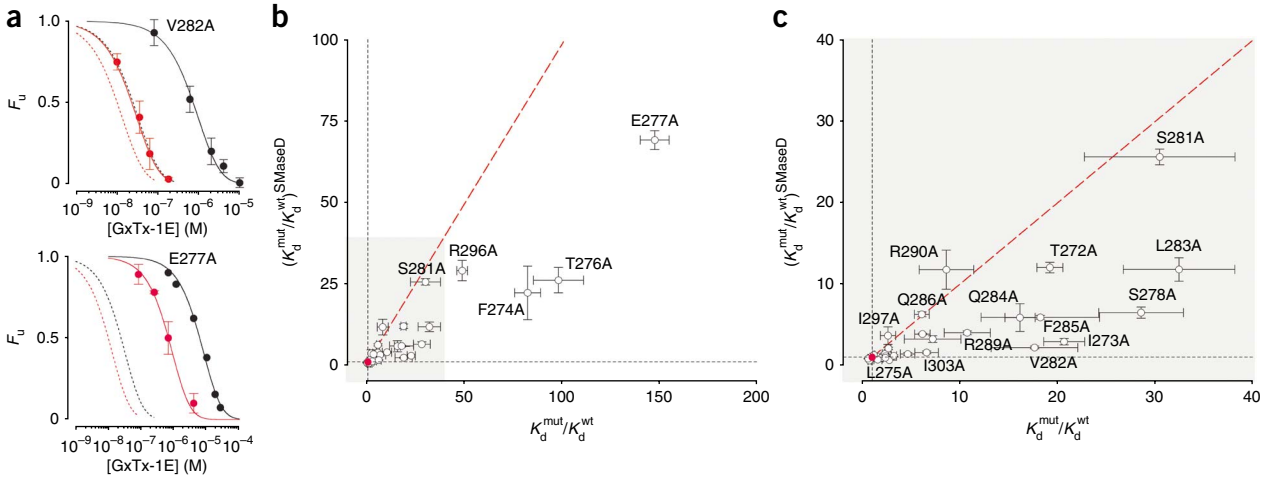

Figure 3 Comparison of the effects of Kv2.1 paddle mutations on GxTx-1E affinity before and after membrane modification with SMaseD. (**a**) Concentration dependence for GxTx-1E occupancy of V282A and E277A mutants of Kv2.1 before (black) and after (red) SMaseD treatment. The apparent K_d values are 3.8 ± 0.4 μM and 120 ± 9 nM for V282A and 30 ± 1.5 μM and 3.5 ± 0.15 μM for E277A. Dashed lines represent the fits for the wild-type channel data from **Figure 2a**. (**b**,**c**) Effects of mutations on toxin affinity (K_d^{mut}/K_d^{wt}) for control membranes plotted against that following treatment with SMaseD. The value for the wild-type channel is indicated by the red circle. The red dotted line corresponds to identical perturbations for control and SMaseD-treated membranes (no coupling between the mutation and the lipid modification). Data from **Supplementary Table 1**. Each mutant was examined initially using a concentration of toxin near the K_d for the wild type; mutants with different K_d were further examined using a wider range of concentrations. n = 3; error bars are s.e.m.

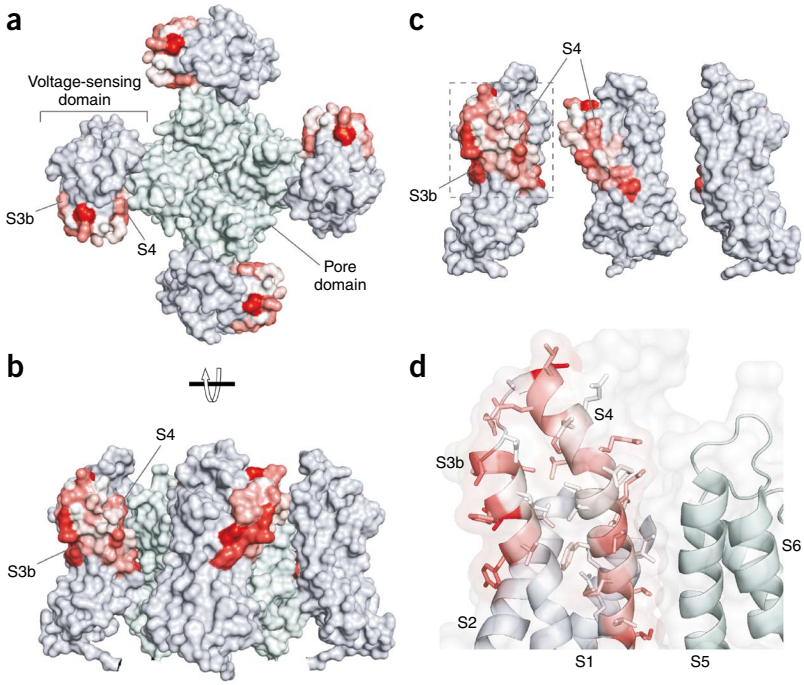

Figure 4 Coupling energies mapped onto the X-ray structure of a Kv channel (PDB 2R9R)[41] and a model for how lipid modification alters toxin affinity. (**a**) Surface representation of the Kv2.1–Kv1.2 paddle chimera with coupling energies mapped onto the paddle region, viewed from the extracellular side of the membrane. A color gradient between white and red was used to represent increasing |Δ*G*| values from 0 to 1.3 kcal mol^{-1}. Residues in the pore domain are colored light cyan and those in the S1–S4 domains outside the paddle motif are colored light blue. (**b**) Surface representation of the Kv2.1–Kv1.2 paddle chimera viewed from the side. (**c**) Surface representation of the Kv2.1–Kv1.2 paddle chimera viewed from the side with the front S1–S4 voltage-sensing domain and central pore domain removed. (**d**) Close-up view of the S3b–S4 paddle motif with transparent surfaces and side chains colored as in **a**. Residues in the S1–S2 loop were removed for clarity and all structures were drawn using PyMol (DeLano Scientific).

be evaluated for all mutations by plotting the mutation-induced perturbation in toxin affinity for control membranes (K_d^{mut}/K_d^{wt}) against that for SMaseD-treated membranes (**Fig. 3b**,**c**). F285A, I273A, S278A and L283A are examples where the lipid modification largely corrects the weakening of toxins affinity, as described above for V282A. In other cases, the effects of the mutations are unaltered by lipid modification, regardless of whether the effects of the mutation on toxin affinity are small (for example, I297A, Q286A and R290A) or large (for example, S281A and R296A), indicating that there is specificity in the coupling between the lipid modification and the paddle mutations.

To understand where on the paddle motif these lipid interactions occur, we calculated the free energy associated with the coupling between channel mutations and the lipid modification[34,35] ($\Delta G_{coupling}$; **Supplementary Fig. 2**) and mapped them onto the X-ray structure of the Kv2.1–Kv1.2 paddle chimera[1], a structure in which the voltage sensor is activated and the pore is open. Using a continuous color gradient between white and red to represent increasing $|\Delta G_{coupling}|$, we can see that mutations that are coupled with the lipid modification tend to concentrate in two regions of the paddle motif (**Fig. 4**). The first is on the surface of the S3b helix that projects out toward the surrounding bilayer (**Fig. 4a**,**b**), and the second is on the surface of the S4 helix facing the S5 helix from the adjacent subunit (**Fig. 4c**). Residues at the interface between the S3b and S4 helices are notable in that their mutation does not couple to the lipid modification (**Fig. 4d**). Further experiments using VSTx1 as a detector to measure coupling between S4 mutations in the KvAP[S4] chimera and lipid modification identify a similar face of the S4 helix where coupling occurs (**Supplementary Figs. 3** and **4** and **Supplementary Table 3**), demonstrating that lipids can interact with similar regions of S4 in distantly related Kv channels.

DISCUSSION

The goal of the present study was to explore the interaction of sphingomyelin with S1–S4 voltage-sensing domains and the role of the lipid in the function and pharmacology of Kv channels. Our experiments with Ci-VSP establish that modification of sphingomyelin can influence the S1–S4 voltage-sensing domains in the absence of a pore domain (**Fig. 1b**), and the results with paddle chimeras point to interactions between the lipid and the paddle motif (**Fig. 2**). In testing the idea that sphingomyelin may act similarly to a non-annular lipid and bind to the paddle motif, we investigated whether tarantula toxins can sense modification of the lipid. SMaseD treatment typically increases the apparent affinity of these toxins, but the extent varies greatly for different toxin-paddle combinations (**Fig. 2**) and, in particular, for mutations on the paddle motif of Kv2.1 (**Fig. 3**). The lipid modification does not influence the interaction of the toxin with the bulk membrane (**Fig. 2**), suggesting that toxin detects a local alteration near where it binds to the paddle motif. These results demonstrate that the pharmacological sensitivity of an ion channel can be profoundly influenced by the identity of lipids around the channel and their interactions with specific structural motifs.

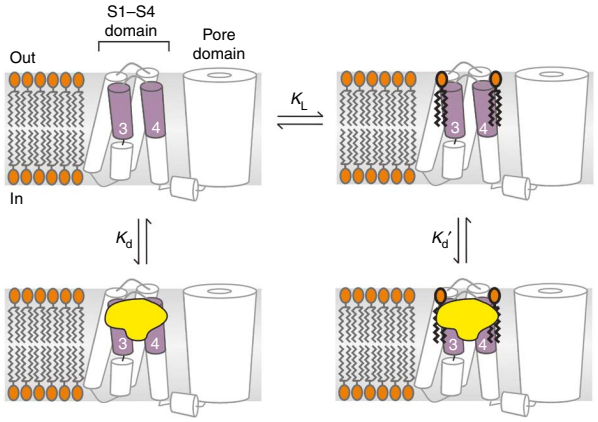

Figure 5 Model illustrating toxin binding to lipid-associated paddle motifs. Lipids are depicted as binding and unbinding from the paddle motif, and toxin affinity is higher for paddle motifs with lipids bound ($K_d' < K_d$). Conversion of sphingomyelin to ceramide-1-phosphate could enhance toxin affinity either because the modified lipid binds more strongly (lower K_L) or because the toxin binds more strongly to paddles interacting with ceramide-1-phosphate than to paddles interacting with sphingomyelin.

How does the modification of sphingomyelin alter the sensitivity of Kv2.1 to tarantula toxins? It seems likely that the effects of SMaseD are not simply the consequence of removing sphingomyelin, because conversion of the lipid to either ceramide-1-phosphate with SMaseD or to ceramide with SMaseC has different effects on the gating of Kv2.1. The former facilitates opening[6] (**Fig. 1**), whereas the latter creates a barrier to opening of the channel[7]. It is unlikely that the effects of the lipase on toxin affinity are secondary to the dissociation of sphingomyelin-rich lipid microdomains (rafts) because mutations in the paddle motif couple with the lipid modification (**Fig. 3**). In addition, dissociation of these microdomains with cholesterol depletion does not influence activation of Kv2.1 channels[6,36] or sensitivity of the channel to tarantula toxins (not shown). One way to explain the effect of lipid modification on toxin affinity would be to postulate that tarantula toxins bind to the paddle motif with higher affinity when sphingomyelin is bound (**Fig. 5**; $K_d' < K_d$)). In this way, mutations could weaken toxin binding by disrupting lipid-paddle interactions, rather than by altering a protein-protein interaction between toxin and channel (**Fig. 3a**). In the context of this model, lipid modification could rescue high-affinity toxin binding after mutations weaken lipid-paddle interactions either because the interaction of the modified lipid is stronger (lower K_L) or because the toxin binds more strongly to paddles interacting with ceramide-1-phosphate than to paddles interacting with sphingomyelin.

Where on the paddle motif do the lipids bind? Our experiments using tarantula toxins as detectors uncovered surfaces of both the S3b and S4 helices within the paddle motif where mutations couple with the lipid modification (**Fig. 4**). Interactions between lipids and the S3b helix are interesting because these might help to anchor the helix near the membrane surface, which would be consistent with studies showing that residues in S3b do not show substantial changes in accessibility to water-soluble agents during gating[37–39]. Interaction of lipids with the surface of S4 that faces S5 is an ideal location to maximize electrostatic interactions between phosphate lipid head groups and the outer S4 arginine residues to stabilize the voltage sensor in an activated state[5–7]. These protein-lipid interactions at the interface between the voltage-sensing and pore domains could explain why S5 mutants in this region can hinder voltage sensor activation[40], even though the S4 and S5 helices do not pack together tightly in X-ray structures[1,41]. The presence of bound lipids between S4 and S5 is consistent with the general picture whereby non-annular lipids bind to membrane proteins at interfaces between transmembrane helices[13,14]. Although structural information on sphingolipid-binding proteins is limited, helix-turn-helix motifs reminiscent of the paddle motifs found in voltage sensors have been proposed to bind these lipids[42,43].

Our observations concerning the sensitivity of Kv channel pharmacology to lipids fit nicely with the discovery that Kv channel pharmacology can also be modulated by the mechanical properties of the membrane[10]. The important implication is that the pharmacology of the ion channel is not determined by the protein alone, but by the lipids in the surrounding membrane and how they interact with the channel protein. It will be fascinating to explore whether variations in the composition and properties of membranes in different subcellular compartments, cell types or pathophysiological conditions influence the gating properties and pharmacological sensitivities of voltage-activated ion channels.

METHODS

Methods and any associated references are available in the online version of the paper at http://www.nature.com/nsmb/.

Note: Supplementary information is available on the Nature Structural & Molecular Biology website.

ACKNOWLEDGMENTS

We thank M. Holmgren, J. Kumar, M. Mayer, J. Mindell, S. Silberberg and members of the Swartz laboratory for helpful discussions and the US National Institute of Neurological Disorders and Stroke (NINDS) DNA sequencing facility for DNA sequencing. We thank Y. Okamura (Okazaki Center for Integrative Biosciences) for providing Ci-VSP complementary DNA, Y. Xu and Z. Lu (University of Pennsylvania) for supplying recombinant SMaseD and W. Schmalhofer and M. Garcia (Merck Research Labs) for supplying ^{125}I-GxTx-1E. This work was supported by the Intramural Research Program of the NINDS, National Insitutes of Health (NIH) (to K.J.S.) and by an NIH-FWO postdoctoral fellowship (to F.B.).

AUTHOR CONTRIBUTIONS

M.M., F.B. and A.A.A. performed molecular biology and electrophysiology experiments, and S.L. synthesized GxTx-1E. All authors contributed to the study design and to writing the manuscript.

Published online at http://www.nature.com/nsmb/.

1. Long, S.B., Tao, X., Campbell, E.B. & MacKinnon, R. Atomic structure of a voltage-dependent K+ channel in a lipid membrane-like environment. *Nature* **450**, 376–382 (2007).
2. Doyle, D.A. *et al.* The structure of the potassium channel: molecular basis of K+ conduction and selectivity. *Science* **280**, 69–77 (1998).
3. Swartz, K.J. Sensing voltage across lipid membranes. *Nature* **456**, 891–897 (2008).
4. Jiang, Y. *et al.* X-ray structure of a voltage-dependent K+ channel. *Nature* **423**, 33–41 (2003).
5. Schmidt, D., Jiang, Q.X. & MacKinnon, R. Phospholipids and the origin of cationic gating charges in voltage sensors. *Nature* **444**, 775–779 (2006).
6. Ramu, Y., Xu, Y. & Lu, Z. Enzymatic activation of voltage-gated potassium channels. *Nature* **442**, 696–699 (2006).
7. Xu, Y., Ramu, Y. & Lu, Z. Removal of phospho-head groups of membrane lipids immobilizes voltage sensors of K+ channels. *Nature* **451**, 826–829 (2008).
8. Alabi, A.A., Bahamonde, M.I., Jung, H.J., Kim, J.I. & Swartz, K.J. Portability of paddle motif function and pharmacology in voltage sensors. *Nature* **450**, 370–375 (2007).
9. Milescu, M. *et al.* Tarantula toxins interact with voltage sensors within lipid membranes. *J. Gen. Physiol.* **130**, 497–511 (2007).
10. Schmidt, D. & Mackinnon, R. Voltage-dependent K+ channel gating and voltage sensor toxin sensitivity depend on the mechanical state of the lipid membrane. *Proc. Natl. Acad. Sci. USA* **105**, 19276–19281 (2008).
11. Kamb, A., Tseng-Crank, J. & Tanouye, M.A. Multiple products of the *Drosophila* Shaker gene may contribute to potassium channel diversity. *Neuron* **1**, 421–430 (1988).
12. Frech, G.C., VanDongen, A.M., Schuster, G., Brown, A.M. & Joho, R.H. A novel potassium channel with delayed rectifier properties isolated from rat brain by expression cloning. *Nature* **340**, 642–645 (1989).
13. Palsdottir, H. & Hunte, C. Lipids in membrane protein structures. *Biochim. Biophys. Acta* **1666**, 2–18 (2004).
14. Lee, A.G. Lipid-protein interactions in biological membranes: a structural perspective. *Biochim. Biophys. Acta* **1612**, 1–40 (2003).
15. Murata, Y., Iwasaki, H., Sasaki, M., Inaba, K. & Okamura, Y. Phosphoinositide phosphatase activity coupled to an intrinsic voltage sensor. *Nature* **435**, 1239–1243 (2005).
16. Villalba-Galea, C.A., Sandtner, W., Starace, D.M. & Bezanilla, F. S4-based voltage sensors have three major conformations. *Proc. Natl. Acad. Sci. USA* **105**, 17600–17607 (2008).
17. Villalba-Galea, C.A., Miceli, F., Taglialatela, M. & Bezanilla, F. Coupling between the voltage-sensing and phosphatase domains of Ci-VSP. *J. Gen. Physiol.* **134**, 5–14 (2009).
18. Cuello, L.G., Cortes, D.M. & Perozo, E. Molecular architecture of the KvAP voltage-dependent K+ channel in a lipid bilayer. *Science* **306**, 491–495 (2004).
19. Ruta, V., Chen, J. & MacKinnon, R. Calibrated measurement of gating-charge arginine displacement in the KvAP voltage-dependent K+ channel. *Cell* **123**, 463–475 (2005).
20. Banerjee, A. & MacKinnon, R. Inferred motions of the S3a helix during voltage-dependent K+ channel gating. *J. Mol. Biol.* **381**, 569–580 (2008).
21. Bosmans, F., Martin-Eauclaire, M.F. & Swartz, K.J. Deconstructing voltage sensor function and pharmacology in sodium channels. *Nature* **456**, 202–208 (2008).
22. Chakrapani, S., Cuello, L.G., Cortes, D.M. & Perozo, E. Structural dynamics of an isolated voltage-sensor domain in a lipid bilayer. *Structure* **16**, 398–409 (2008).
23. Trimmer, J.S. *et al.* Primary structure and functional expression of a mammalian skeletal muscle sodium channel. *Neuron* **3**, 33–49 (1989).

24. Lee, S.Y. & MacKinnon, R. A membrane-access mechanism of ion channel inhibition by voltage sensor toxins from spider venom. *Nature* **430**, 232–235 (2004).
25. Jung, H.J. *et al.* Solution structure and lipid membrane partitioning of VSTx1, an inhibitor of the KvAP potassium channel. *Biochemistry* **44**, 6015–6023 (2005).
26. Phillips, L.R. *et al.* Voltage-sensor activation with a tarantula toxin as cargo. *Nature* **436**, 857–860 (2005).
27. Swartz, K.J. & MacKinnon, R. Mapping the receptor site for hanatoxin, a gating modifier of voltage-dependent K^+ channels. *Neuron* **18**, 675–682 (1997b).
28. Li-Smerin, Y., Hackos, D.H. & Swartz, K.J. α-Helical structural elements within the voltage-sensing domains of a K^+ channel. *J. Gen. Physiol.* **115**, 33–50 (2000a).
29. Li-Smerin, Y. & Swartz, K.J. Helical structure of the COOH terminus of S3 and its contribution to the gating modifier toxin receptor in voltage-gated ion channels. *J. Gen. Physiol.* **117**, 205–218 (2001).
30. Herrington, J. *et al.* Blockers of the delayed-rectifier potassium current in pancreatic β-cells enhance glucose-dependent insulin secretion. *Diabetes* **55**, 1034–1042 (2006).
31. Ruta, V., Jiang, Y., Lee, A., Chen, J. & MacKinnon, R. Functional analysis of an archaebacterial voltage-dependent K^+ channel. *Nature* **422**, 180–185 (2003).
32. Middleton, R.E. *et al.* Two tarantula peptides inhibit activation of multiple sodium channels. *Biochemistry* **41**, 14734–14747 (2002).
33. Li-Smerin, Y. & Swartz, K.J. Localization and molecular determinants of the hanatoxin receptors on the voltage-sensing domain of a K^+ channel. *J. Gen. Physiol.* **115**, 673–684 (2000).
34. Hidalgo, P. & MacKinnon, R. Revealing the architecture of a K^+ channel pore through mutant cycles with a peptide inhibitor. *Science* **268**, 307–310 (1995).
35. Schreiber, G. & Fersht, A.R. Energetics of protein-protein interactions: analysis of the barnase-barstar interface by single mutations and double mutant cycles. *J. Mol. Biol.* **248**, 478–486 (1995).
36. Martens, J.R. *et al.* Differential targeting of Shaker-like potassium channels to lipid rafts. *J. Biol. Chem.* **275**, 7443–7446 (2000).
37. Nguyen, T.P. & Horn, R. Movement and crevices around a sodium channel S3 segment. *J. Gen. Physiol.* **120**, 419–436 (2002).
38. Gandhi, C.S., Clark, E., Loots, E., Pralle, A. & Isacoff, E.Y. The orientation and molecular movement of a K^+ channel voltage-sensing domain. *Neuron* **40**, 515–525 (2003).
39. Darman, R.B., Ivy, A.A., Ketty, V. & Blaustein, R.O. Constraints on voltage sensor movement in the Shaker K^+ channel. *J. Gen. Physiol.* **128**, 687–699 (2006).
40. Soler-Llavina, G.J., Chang, T.H. & Swartz, K.J. Functional interactions at the interface between voltage-sensing and pore domains in the Shaker K_v channel. *Neuron* **52**, 623–634 (2006).
41. Long, S.B., Campbell, E.B. & Mackinnon, R. Crystal structure of a mammalian voltage-dependent Shaker family K^+ channel. *Science* **309**, 897–903 (2005).
42. Mahfoud, R. *et al.* Identification of a common sphingolipid-binding domain in Alzheimer, prion, and HIV-1 proteins. *J. Biol. Chem.* **277**, 11292–11296 (2002).
43. Snook, C.F., Jones, J.A. & Hannun, Y.A. Sphingolipid-binding proteins. *Biochim. Biophys. Acta* **1761**, 927–946 (2006).

ONLINE METHODS

Electrophysiological recording. We carried out expression of Kv channel and Ci-VSP constructs in *Xenopus laevis* oocytes and studied them using two-electrode voltage-clamp recording techniques (OC-725C, Warner Instruments) as described[33]. Data were filtered at 1 kHz and digitized at 10 kHz. Microelectrode resistances were 0.1–1 MΩ when filled with 3M KCl. For ionic current measurements, the external recording solution contained 50 mM KCl, 50 mM NaCl, 5 mM HEPES, 1 mM $MgCl_2$ and 0.3 mM $CaCl_2$, pH 7.6 (with NaOH). For gating current measurements on Ci-VSP, the external recording solution contained 100 mM NaCl, 10 mM HEPES, 1 mM $MgCl_2$ and 0.3 mM $CaCl_2$, pH 7.6 (with NaOH). Recombinant SMaseD (final concentration 8 ng μl^{-1}) was added to the recording chamber for 10–15 min, as described[6], using weak depolarizations elicited at 3-s intervals to monitor the effects of the enzyme. After reaching equilibrium, the oocyte was washed extensively with the recording solution. We performed all experiments at room temperature (~22 °C). We synthesized GxTx-1E and VSTx1 using solid-phase chemical methods, as described[25] and purchased ProTx-I from Peptides International. We obtained conductance-voltage relations from tail currents measured after a series of membrane depolarizations. For a few mutants that showed fast deactivation kinetics, we calculated conductance from steady-state current measurements.

Estimating toxin occupancy of channels. We examined the occupancy of closed or resting channels by toxins using negative holding voltages where the open probability is low, and we estimated the fraction of unbound channels (F_u) using depolarizations that are too weak to open toxin-bound channels (**Supplementary Fig. 5**), as described[26,27,29,33,44,45]. For all channels, we recorded voltage-activation relationships in the absence and presence of different concentrations of toxin. We calculated the ratio of currents (I/I_0) recorded in the presence (I) and absence (I_0) of toxin for various strength depolarizations, typically −70 mV to +10 mV, and the value of I/I_0 measured in the plateau phase at voltages where toxin-bound channels do not open was taken as F_u (**Supplementary Fig. 5**). For all the experiments, voltage protocols were adjusted appropriately so that the plateau phase in the I/I_0-voltage relationship was well defined. The apparent K_d was calculated assuming four independent toxin-binding sites per channel, with single occupancy being sufficient to inhibit opening in response to weak depolarizations: $K_d = ((1/(1 - F_u^{1/4})) - 1)$ [Toxin].

Toxin partitioning into oocytes membranes. We incubated 20 defolliculated *X. laevis* oocytes at room temperature (~22 °C) in a solution (350 µl) containing 50 mM KCl, 50 mM NaCl mM, 5 mM HEPES, 1 mM $MgCl_2$, 0.3 mM $CaCl_2$, pH 7.6 (with NaOH) and 200 nM ^{125}I-GxTx-1E (20 Ci $mmol^{-1}$; provided by W. Schmalhofer and M. Garcia). After 15 min, we separated the oocytes by decantation, washed them twice with 1 ml of ice-cold solution without GxTx-1E and measured the amount of radiolabeled toxin in a liquid scintillation counter. To examine the effect of lipid modification on toxin partitioning into lipid membranes, we pre-incubated oocytes for 30 min with SMaseD (20 ng μl^{-1}). The fraction partitioned (f_p) was calculated as $f_p = [toxin_{bound}]/[toxin_{total}]$.

44. Swartz, K.J. & MacKinnon, R. Hanatoxin modifies the gating of a voltage-dependent K^+ channel through multiple binding sites. *Neuron* **18**, 665–673 (1997a).
45. Lee, H.C., Wang, J.M. & Swartz, K.J. Interaction between extracellular Hanatoxin and the resting conformation of the voltage-sensor paddle in Kv channels. *Neuron* **40**, 527–536 (2003).

doi:10.1038/nsmb.1679